Radio Science, Volume 34, Number 2, Pages 297–309, March–April 1999

State-space formulation of two-dimensional electromagnetic scattering from dielectric cylinders

Naser A. Abu Zaid, Abdullah Y. Niazi, and Haluk Tosun

Department of Electrical and Electronic Engineering, Eastern Mediterranean University, Mersin, Turkey

Abstract. A numerical method is presented for the problem of transverse magnetic or transverse electric scattering from infinitely long, lossy dielectric cylinders of arbitrary cross section. The method is based on the solution of a system of linear ordinary differential equations in the state-space form. The solution is achieved by finding the state transition-matrix and the zero-state response of the respective system. Numerical results are presented for cylinders of various cross sections, and they are compared with the results obtained by either exact or approximate numerical methods.

1. Introduction

There have been various numerical approaches to the problem of electromagnetic scattering by dielectric cylinders of arbitrary cross section, among which may be cited the well-known moment method [*Richmond*, 1965], the conformal mapping solution [*Shafai*, 1970], the phase and amplitude functions solution [*Shafai*, 1971], the unimoment method [*Change and Mei*, 1976], the coupled surface integral equations method [*Wu and Tsai*, 1977], the mode-matching method [*Okuni*, 1990], and the equivalent source method [*Shigesawa*, 1990]. *Richmond* [1965] *and Wu and Tsai* [1977] solved the relevant integral equations numerically by discretization and matrix inversion. *Shafai* [1971] defined suitable phase and amplitude functions (which are related to the unknown radial functions of the infinite series representation of the fields) and numerically solved them to find the unknown fields. The unimoment method is a combined solution of an internal finite element problem and an external cylindrical harmonic expansion [*Okuni*, 1990; *Shigesawa*, 1990] and are essentially generalized multipole techniques. Recently, some new ways of solving the dielectric scattering problem were published [*Riechers*, 1990; *Leviatan and Boag*, 1988; *Cangellaris and Lee*, 1990; *Tosun*, 1994].

Paper number 1998RS900001.
0048-6604/99/1998RS900001$11.00

The method of solution presented here may be called the state-space method because of its similarity to a more general three-dimensional vector scattering problem [*Hizal and Tosun*, 1973]. It is essentially a polarization-source formulation [*Bates*, 1972] in which the volume induction theorem is the starting point.

In state-space formulation, the fields are represented by an infinite series of cylindrical harmonics with position-dependent expansion coefficients. The infinite-dimensional system of differential equations for these coefficients is next projected into a finite-dimensional subspace, and the resultant system acquires a state-space form. This procedure yields a finite-dimensional two-point boundary value problem whose solution is achieved with the well-known techniques of linear system theory.

The excitation is chosen to be a uniform plane wave or a line source parallel to the cylinder axis. The formulation is done for both transverse magnetic and transverse electric polarizations but numerical results are given only for the TM case. The material parameters of the scatterer (σ,ε) are allowed to vary over the cross section but not with the axial distance.

With the widespread availability of really powerful computational techniques, the electromagnetic scattering problem is no longer an unsolvable one. Yet novel ways of solving such problems seem to maintain continuous popularity in the related literature. We hope in this respect that the method proposed in this paper will have a similar role.

2. Formulation

2.1. TM Excitation Case

We consider an infinitely long dielectric cylinder with an arbitrary cross section, as shown in Figure 1. A TM-polarized plane wave is incident on the scatterer with an angle ψ_o with respect to the $+x$ axis. We denote the cross-sectional surface of the cylindrical scatterer by A and denote its boundary contour by C.

The scatterer is assumed to be nonmagnetic, so $\mu = \mu_o$ everywhere. The scattered field E_z^s due to the induced conduction and polarization currents can be written as [*Harrington*, 1961] (time dependence is $e^{j\omega t}$)

$$E_z^s(\rho,\phi) = -\frac{k_o Z_o}{4}\iint_A J_{eq}(\rho',\phi')H_o^{(2)}(k_o R)dA' \quad (1)$$

where (ρ,ϕ) are the cylindrical coordinates of the observation point, (ρ',ϕ') are those for the source point on the cross section of the cylinder, k_o is the free-space wave number, $k_o = \omega\sqrt{\varepsilon_o\mu_o}$, $Z_o = 120\pi(\Omega)$, and $H_o^{(2)}$ is the zeroth-order Hankel function of second kind,

$$R = \left[\rho^2 + \rho'^2 - 2\rho\rho'\cos(\phi-\phi')\right]^{1/2}$$

$$J_{eq}(\rho,\phi) = j\omega\varepsilon'\left[E_z^i(\rho,\phi) + E_z^s(\rho,\phi)\right]$$

$$\varepsilon' = \varepsilon - \varepsilon_o - j\frac{\sigma}{\omega}$$

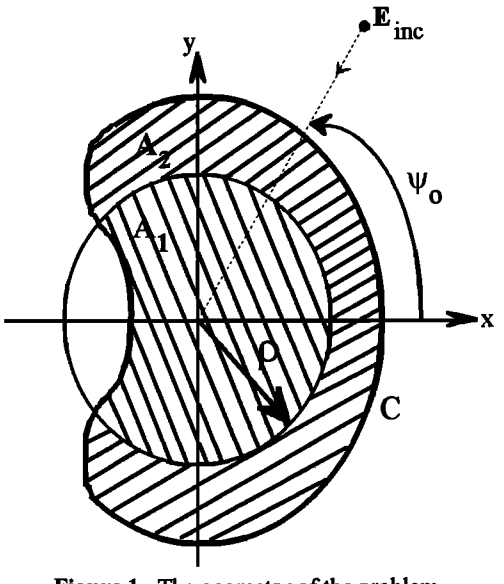

Figure 1. The geometry of the problem.

Equation (1) is valid everywhere, that is, for (ρ,ϕ) located both inside and outside C. If we locate (ρ,ϕ) somewhere in C, (1) can be written as

$$E_z^s(\rho,\phi) = -\frac{k_o Z_o}{4}\sum_{i=1}^{2}\iint_{A_i} J_{eq}(\rho',\phi')H_o^{(2)}(k_o R)dA', \quad \begin{cases} 0 \le \rho < \infty \\ 0 \le \phi \le 2\pi \end{cases} \quad (2)$$

where, on A_1, ρ'<ρ, and on A_2, ρ<ρ' and $A_1 \cup A_2 = A$. The partitioning of the surface integral in (1) into two parts in (2) is legitimate because this is actually equivalent to decomposing the support of J_{eq} into two complementary sections. Now, if the addition theorem for the Hankel function, namely,

$$H_o^2(k_o R) = \begin{cases} \sum_{m=-\infty}^{\infty} J_m(k_o\rho')H_m^{(2)}(k_o\rho)e^{jm(\phi-\phi')}, & \rho' < \rho \\ \sum_{m=-\infty}^{\infty} J_m(k_o\rho)H_m^{(2)}(k_o\rho')e^{jm(\phi-\phi')}, & \rho' > \rho \end{cases}$$

is used in (2), we get

$$E_z^s(\rho,\phi) = \sum_{i=1}^{2}\sum_{m=-\infty}^{\infty} S_m^i(\rho)Z_m^p(k_o\rho)e^{jm\phi} \quad (3)$$

where $p = 1+\delta_{i1}$; δ_{ij} is the Kronecker delta; $Z_m^1(k_o\rho) = J_m(k_o\rho)$ is the Bessel function of first kind, mth order; and $Z_m^2(k_o\rho) = H_m^{(2)}(k_o\rho)$. In the addition theorem, when $\rho = \rho'$, the series must diverge if they reliably represent $H_o^{(2)}(k_o R)$, because $\rho = \rho'$ means R=0, and $H_o^{(2)}(k_o R)$ has a singularity there. However, $H_o^{(2)}(k_o R)$ has a removable singularity in (1) since the rate of decrease of the area element is greater than the rate of increase of $H_o^{(2)}(k_o R)$. In obtaining (3), the order of integration and summation operators has been interchanged. The validity of this is based on the fact that the series in the addition theorem are uniformly convergent in the variable ρ'.

$S_m^i(\rho)$ in (3) are called the scattering coefficients, defined by

$$S_m^i(\rho) = -\frac{k_o Z_o}{4}\iint_{A_i} J_{eq}(\rho',\phi')Z_m^i(k_o\rho')e^{-jm\phi'}dA' \quad (4)$$

where i=1 or 2. Since

$$J_{eq}(\rho,\phi) = j\omega\varepsilon'\left[E_z^i(\rho,\phi) + E_z^s(\rho,\phi)\right]$$

using (3) for E_z^s, we can represent it as

$$J_{eq}(\rho,\phi) = j\omega\varepsilon'\left[E_z^i(\rho,\phi) + \sum_{q=1}^{2}\sum_{m=-\infty}^{\infty} S_m^q(\rho) Z_m^p(k_o\rho) e^{jm\phi}\right] \tag{5}$$

with $p = 1+\delta_{q1}$.

On the other hand, the electric field of the incident wave has the following series expansion in terms of cylindrical harmonics:

$$E_z^i(\rho,\phi) = \sum_{m=-\infty}^{\infty} e_m J_m(k_o\rho) e^{jm\phi} \tag{6}$$

where

$$e_m = j^m e^{-jm\phi_o}$$

for plane wave (of unit amplitude) incidence, and

$$e_m = -\frac{k_o Z_o}{4} H_m^{(2)}(k_o D) e^{-jm\phi_o}$$

for line source (of unit amplitude) located at (D,ϕ_o).

(Here we assume $D \rangle \rho_2$ = enscribing radius, that is, the smallest radius of a circle touching the cross section from outside).

When (6) is used in (5), there results the following representation for J_{eq}:

$$J_{eq}(\rho,\phi) = \sum_{q=1}^{2}\sum_{m=-\infty}^{\infty}\left[S_m^q(\rho) Z_m^p(k_o\rho) + e_m Z_m^q(k_o\rho)\delta_{q1}\right] e^{jm\phi} \tag{7}$$

Next, we substitute (7) into (4), with the result

$$S_m^k(\rho) = -\frac{k_o Z_o}{4}\iint_{A_k} j\omega\varepsilon'\left\{\sum_{q=1}^{2}\sum_{n=-\infty}^{\infty}\left[S_n^q(\rho') Z_n^p(k_o\rho') + e_n Z_n^q(k_o\rho')\delta_{q1}\right] e^{jn\phi'}\right\} Z_m^k(k_o\rho') e^{-jm\phi'} dA' \tag{8}$$

Since A_k depends on ρ, i.e.,

$$\iint_{A_1}.....dA' = \int_0^{\rho}\int_{\phi(\rho')}.....\rho' d\rho' d\phi' \text{ and } \iint_{A_2}.....dA' = \int_{\rho}^{\rho_2}\int_{\phi(\rho')}.....\rho' d\rho' d\phi'$$

equation (8) represents a system of integral equations of Volterra type for the unknown expansion coefficients $S_m^k(\rho)$, for k=1 and 2. This can be converted to a system of linear differential equations by differentiating both sides of (8) with respect to ρ. The result is

$$\frac{dS_m^k}{d\rho} = \sum_{q=1}^{2}\sum_{n=-\infty}^{\infty}\left[W_{nm}^{kq}(\rho) S_n^q(\rho) + e_n W_{nm}^{kq}(\rho)\delta_{q1}\right] \tag{9}$$

where the functions $W_{nm}^{kq}(\rho)$ are defined as

$$W_{nm}^{kq}(\rho) = (-1)^k \frac{jk_o^2}{4}\rho Z_n^p(k_o\rho) Z_m^k(k_o\rho) I_{nm}(\rho) \tag{10}$$

with $p = 1+\delta_{q1}$ and

$$I_{nm}(\rho) = \int_{\Phi(\rho)} \frac{\varepsilon'}{\varepsilon_o} e^{j(n-m)\phi} d\phi \tag{11}$$

We call I_{nm} shape factors. To see how they arise in (10), we refer to (8) and rewrite it explicitly as (say, for k=1)

$$S_m^1(\rho) = -\frac{k_o Z_o}{4}\int_0^{\rho}\int_{\phi(\rho')} j\omega\varepsilon'\left\{\sum_{n=-\infty}^{\infty}\left[S_n^1(\rho') H_n^{(2)}(k_o\rho') + S_n^2(\rho') J_n(k_o\rho') + e_n J_n(k_o\rho')\right]\right\} J_m(k_o\rho') e^{j(n-m)\phi'}\rho' d\rho' d\phi'$$

or

$$S_m^1(\rho) = -\frac{k_o Z_o}{4}\sum_{n=-\infty}^{\infty}\int_0^{\rho} f_{nm}(\rho')\rho' d\rho' \int_{\phi(\rho')} j\omega\varepsilon' e^{j(n-m)\phi'} d\phi' \tag{12}$$

where

$$f_{nm}(\rho') = \left[S_n^1(\rho') H_n^2(k_o\rho') + S_n^2(\rho') J_n(k_o\rho') e_n J_n(k_o\rho')\right] J_m(k_o\rho')$$

Now differentiating both sides of (12) with respect to ρ gives

$$\frac{dS_m^1(\rho)}{d\rho} = -\frac{k_o Z_o}{4}\sum_{n=-\infty}^{\infty} f_{nm}(\rho)\rho \int_{\phi(\rho)} j\omega\varepsilon' e^{j(n-m)\phi'} d\phi' \tag{13}$$

from which (9) follows immediately for k=1. The case where k=2 is similar. We calculate I_{nm} with reference to Figure 2 as follows:

$$I_{nm}(\rho) = \int_{\phi_2}^{\phi_3} \varepsilon'_r e^{j(n-m)\phi} d\phi + \int_{\phi_4}^{\phi_1} \varepsilon'_r e^{j(n-m)\phi} d\phi \tag{14}$$

where $\varepsilon'_r = \varepsilon'/\varepsilon_o$.

In (14), ε'_r can be allowed to vary with respect to ρ and ϕ. I_{nm} contain the shape information about the scatterer. For example, for an elliptic cross section (of semimajor and semiminor lengths a and b, respectively), I_{nm} will take the form (assuming ε'_r constant over A)

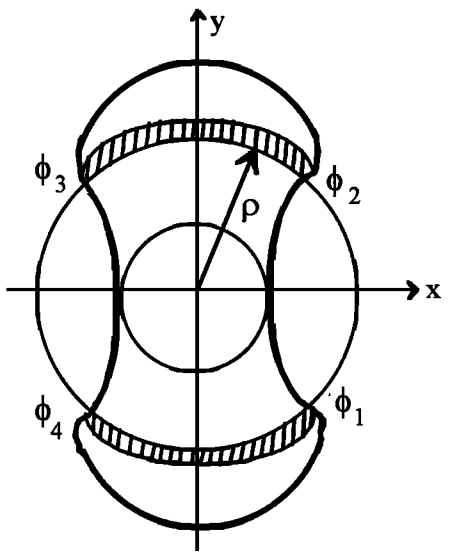

Figure 2. The definition of the shape factors.

$$I_{nm}(\rho)=\begin{cases} 2\pi\varepsilon'_r\,\delta_{nm}, & \rho<\rho_1 \\ 2\varepsilon'_r\left(\pi\delta_{nm}-\left[1+(-1)^{(n-m)}\right]\dfrac{\sin[(n-m)\phi]}{(n-m)}\right), & \rho_1<\rho<\rho_2 \end{cases}$$

where

$$\phi=\frac{1}{2}\arccos\left[\frac{A}{\rho^2}+B\right],\quad \text{with}\quad \begin{cases} A=\dfrac{2a^2b^2}{b^2-a^2} \\ B=\dfrac{a^2+b^2}{a^2-b^2} \end{cases}$$

When the infinite series in (9) is truncated at a finite number N, there results a linear system of differential equations of finite order in the state-space form. It is obvious from (4) that

$$\begin{aligned} S_m^1(0)&=0 \qquad S_m^2(0)\neq 0 \\ S_m^1(\rho_2)&\neq 0 \quad S_m^2(\rho_2)=0 \end{aligned} \tag{15}$$

Since the conditions on s_m^i are specified at two different points, the resultant problem is actually a two-point boundary value problem.

2.2. TE Excitation Case

If the incident radiation is a plane wave having a transverse **E** field and a z-directed **H** field, the wave equation for the scattered magnetic field can be shown to have the following form:

$$\nabla_t^2 H_z^s+k_o^2 H_z^s=-k_o^2\tau H_z+\left(\frac{\partial\ln\eta}{\partial\rho}\frac{\partial H_z}{\partial\rho}+\frac{1}{\rho^2}\frac{\partial\ln\eta}{\partial\phi}\frac{\partial H_z}{\partial\phi}\right) \tag{16}$$

where H_z^s is the scattered field, H_z is the total field, and

$$\tau=\frac{\varepsilon}{\varepsilon_o}-1-j\frac{\sigma}{\omega\varepsilon_o}$$

$$\eta=\varepsilon-j\frac{\sigma}{\omega}$$

Defining the operator $\Re$ as

$$\Re=k_o^2\tau-\left(\frac{\partial\ln\eta}{\partial\rho}\frac{\partial}{\partial\rho}+\frac{1}{\rho^2}\frac{\partial\ln\eta}{\partial\phi}\frac{\partial}{\partial\phi}\right) \tag{17}$$

(12) can be written as

$$\nabla_t^2 H_z^s+k_o^2 H_z^s=-\Re H_z \tag{18}$$

where ∇_t denotes the transverse delta operator.

We can write the solution to (14) as

$$H_z^s(\rho,\phi)=\frac{1}{4j}\iint_A \Re H_z(\rho',\phi')H_o^{(2)}(k_oR)dA' \tag{19}$$

where R and $H_o^{(2)}(k_oR)$ have the same meaning as for the TM case. Using the addition theorem for $H_o^{(2)}(k_oR)$ in (15) results in the following infinite series representation for H_z^s:

$$H_z^s(\rho,\phi)=\sum_{i=1}^{2}\sum_{m=-\infty}^{\infty}S_m^i(\rho)Z_m^p(k_o\rho)e^{jm\phi} \tag{20}$$

where

$$S_m^i(\rho)=\frac{1}{4j}\iint_{A_i}\Re H_z(\rho',\phi')Z_m^t(k_o\rho')e^{-jm\phi'}dA' \tag{21}$$

The linear system of differential equations for $S_m^i(\rho)$ is similarly deduced:

$$\frac{dS_m^k}{d\rho}=\sum_{q=1}^{2}\sum_{n=-\infty}^{\infty}\left[Q_{nm}^{kq}(\rho)S_n^q(\rho)+e_mQ_{nm}^{k2}(\rho)\delta_{q1}\right] \tag{22}$$

where the functions $Q_{nm}^{kp}(\rho)$ are now appropriate for TE excitation and they involve Bessel and Hankel functions, their derivatives and proper shape functions.

The explicit forms of $Q_{nm}^{kq}(\rho)$ are given as

$$Q_{nm}^{kq}(\rho)=(-1)^{k+1}\frac{\rho}{4j}Z_m^q(k_o\rho)I_{nm}^k(\rho)$$

where

$$Z_m^q = J_m(k_o\rho)\delta_{q1} + H_m^{(2)}(k_o\rho)\delta_{q2}$$

$$I_{nm}^q(\rho) = \int_{\Phi(\rho)} Y_n^k(\rho,\phi)e^{j(n-m)\phi}d\phi$$

with

$$Y_n^k(\rho,\phi) = f_n(\rho,\phi)Z_n^r(k_o\rho) + g(\rho,\phi)Z_n^r(k_o\rho)$$

where

$$f_n(\rho,\phi) = k_o^2\tau^* - \frac{jn}{\rho^2}\frac{\partial \ln\eta}{\partial\phi}$$

$$g(\rho,\phi) = -k_o\frac{\partial \ln\eta}{\partial\rho}$$

$$r = 1+\delta_{k1}$$

The conditions on s_m^i are the same as for the TM case.

3. Numerical Solution of the Two-Point Boundary Value Problem

3.1. Solution for the System of Equations

The system of linear differential equations in (9) and (22) can be cast into the following matrix form:

$$\begin{bmatrix}\dot{\mathbf{s}}^1\\ \dot{\mathbf{s}}^2\end{bmatrix} = \begin{bmatrix}\mathbf{Y}^{11} & \mathbf{Y}^{12}\\ \mathbf{Y}^{21} & \mathbf{Y}^{22}\end{bmatrix}\begin{bmatrix}\mathbf{s}^1\\ \mathbf{s}^2\end{bmatrix} + \begin{bmatrix}\mathbf{Y}^{12}\\ \mathbf{Y}^{22}\end{bmatrix}\mathbf{e} \qquad (23)$$

where $\mathbf{s}^1$ and $\mathbf{s}^2$ are $(2N+1)\times 1$ column vectors; $\mathbf{Y}^{ij}$ denote either $\mathbf{W}^{ij}$ or $\mathbf{Q}^{ij}$, depending on whether we have TM or TE excitations, respectively, and they are $(2N+1)\times(2N+1)$ complex square matrices; $\mathbf{e}$ is the $(2N+1)\times 1$ excitation vector whose elements (for the TM case) are $e_n = j^n e^{-jn\psi_o}$ for a plane wave and $e_n = -(k_oZ_o/4)H_n^{(2)}(k_oD)e^{-jn\phi_o}$ for a line source, respectively. Dotted character denote differentiation with respect to x, with $x = k_o\rho$.

The solution to (23) can be written symbolically as

$$\begin{bmatrix}\mathbf{s}^1(x)\\ \mathbf{s}^2(x)\end{bmatrix} = \begin{bmatrix}\Phi_{11}(x) & \Phi_{12}(x)\\ \Phi_{21}(x) & \Phi_{22}(x)\end{bmatrix}\begin{bmatrix}\mathbf{s}^1(0)\\ \mathbf{s}^2(0)\end{bmatrix} + \begin{bmatrix}\mathbf{Z}_1(x)\\ \mathbf{Z}_2(x)\end{bmatrix} \qquad (24)$$

In (24), Φ_{mn} are the state-transition submatrices, $[\mathbf{Z}_1\ \ \mathbf{Z}_2]^T$ is the zero-state response to (23), and T denotes the transpose. To find $[\mathbf{Z}_1\ \ \mathbf{Z}_2]^T$ at any x, (23) is solved numerically from x=0 to x with zero initial condition vector. The columns of the [Φ] matrix are generated by solving (23) with $\mathbf{e}$=0, numerically with the canonical initial condition vectors; that is, to find the jth column of [Φ], we use the initial condition vector $[0\,0....1\,0.....0]^T$, where 1 is at the jth place from the top.

Next, we evaluate (24) at $x=x_2$ and use (15),

$$\begin{bmatrix}\mathbf{s}^1(x_2)\\ \mathbf{0}\end{bmatrix} = \begin{bmatrix}\Phi_{11}(x_2) & \Phi_{12}(x_2)\\ \Phi_{21}(x_2) & \Phi_{22}(x_2)\end{bmatrix}\begin{bmatrix}\mathbf{0}\\ \mathbf{s}^2(0)\end{bmatrix} + \begin{bmatrix}\mathbf{Z}_1(x_2)\\ \mathbf{Z}_2(x_2)\end{bmatrix} \qquad (25)$$

Here $\mathbf{s}^1(x_2)$ and $\mathbf{s}^2(x_1)$ can be obtained by solving (25), with the result

$$\mathbf{s}^1(x_2) = -\Phi_{12}(x_2).\Phi_{22}^{-1}(x_2).\mathbf{Z}_2(x_2) + \mathbf{Z}_1(x_2) \qquad (26)$$

$$\mathbf{s}^2(0) = -\Phi_{22}^{-1}(x_2).\mathbf{Z}_2(x_2) \qquad (27)$$

This completes the solution. For far-field pattern calculations, only $\mathbf{s}^1(x_2)$ is needed. Near-field calculations require $\mathbf{s}^2(0)$ as well.

3.2. Handling the Singularity in the Characteristic Matrix

In generating the matrix [Y] numerically, care must be taken against the singularities that arise in some elements of Yq^k when $x \to 0$. A closer look into (10) shows that W_{nm}^{12} are well behaved near x=0 (the starting point in the solution of the differential equations). Although W_{nm}^{11}, W_{nm}^{21}, and W_{nm}^{22} behave well around x=0 for n=m=0, they show a singular behavior for some values of n and m. This is because W_{nm}^{11}, W_{nm}^{21} and W_{nm}^{22} contain the Hankel functions but W_{nm}^{12} do not. Since S_n^1 are absolutely zero at x=0, the singularity problem is not an analytical one. So it must be handled numerically. This is done by isolating the point x=0 from numerical calculations. The numerical integration in the solution of (23) is to start at a value which is different from zero (if the scatterer is not of a shell shape) but which should be small enough. In actual computations, we chose $x_{\text{initial}} = 10^{-6}$, and this value proved to be quite satisfactory in the sense that beyond this limit down, the final values of the scattering coefficients do not change appreciably.

4. Numerical Applications

4.1. The Method of Solution

What we have obtained in (23) is a system of first-order linear differential equations of size $(4N+2)\times(4N+2)$. To solve this system, the fifth-order Runge-Kutta-Fehlberg method (which integrates the system over the interval x_1 to x_2 with specified initial conditions and self-controlled step size) is used. It should be noted that the final expression for the scattering coefficients, namely, equations (26) and (27), include only the submatrices $[\Phi_{12}(x_2)]$ and $[\Phi_{22}(x_2)]$. This means that instead of generating the whole $[\Phi]$ matrix numerically, we need only half of it. This obviously means a lighter computational burden. If the whole $[\Phi]$ matrix were required, we would solve (23) numerically ($4N$+3) times (($4N$+2) times to generate $[\Phi]$ matrix, one time to obtain the zero-state response vector). Now, however, the solution to (23) is required only ($2N$+2) times (($2N$+1) times, with e=0, to generate half of the $[\Phi]$ matrix, and one time to obtain the zero-state response vector).

4.2. Parameters of Interest

The parameter of interest for describing the far-field behavior of the scatterers is the echo width per wavelength, defined as

$$\frac{\sigma}{\lambda}=\frac{2}{\pi}\left|\sum_{m=-\infty}^{\infty} j^m s_m^1(k_o\rho_2)e^{jm\phi}\right|^2$$

For near-field calculations we consider the magnitude of the **E** field, namely, $|E_z|$, as the parameter of interest.

4.3. Convergence of the Numerical Technique

The scattering parameters are sensitive to the truncation number. It is natural to expect that as the truncation number is increased, the results should tend to be invariant and more correct. This was actually observed numerically on all the examples considered. No effort has been made on the analytical aspects of the convergence problem because this requires a detailed functional analysis on the properties of the operators involved in the solution technique. A priori estimation of the required truncation number and the error bounds in relation to this truncation number are actually fundamental problems in the area of resonant scattering. We believe that any serious attempt in this respect is a very important study in itself. We therefore restricted our work to the numerical tests on the convergence problem. It has been observed that the state-space method is a well convergent one. This was proved to be the case on the numerous examples treated. Some of the convergence results are shown in the respective figures. The question of how fast the method converges depends on the optical size, shape details, and the inhomogeneity of the scatterer. The nearest integer to twice the maximum optical size (physical size of the scatterer cross section in terms of wavelength) can be taken as a measure of the required truncation number. This choice proves to be satisfactory in the sense that increasing the truncation number beyond it has no appreciable effect on the scattering parameters. On the other hand, two scatterers of equal optical size may show different convergence properties depending on the variation of material parameters on their respective cross sections.

It is not easy to make definite statements about comparative computation times for the state-space method and others because different solution techniques are usually tested on different machines, and, most of the time, no detailed computational time behavior is documented. However, it is believed that the state-space method is computationally comparable to the other existing methods.

4.4. Scatterers Considered and Validation

The state-space method was first tested on problems for which exact solutions are available. These include a solid circular dielectric cylinder and a circular dielectric shell. TM wave scattering from such shapes has an exact eigenfunction expansion solution provided that the permittivity is constant over the cross section. Excellent agreement was established between the state-space results and the exact ones. For a circular shell the state-space differential equation system becomes decoupled in the scattering coefficients. A sample result is given in Figure 3.

There have been results in the literature on cross-sectional shapes other than circles. To test the state-space method for a noncircular cross-sectioned cylinder, we took again a circular cross section, but this time we located the coordinate origin not at the center of the circle but somewhere off center. Since this problem has an exact solution, we found it to be representative enough for a meaningful comparison. The exact and state-space results are compared in Figure 4.

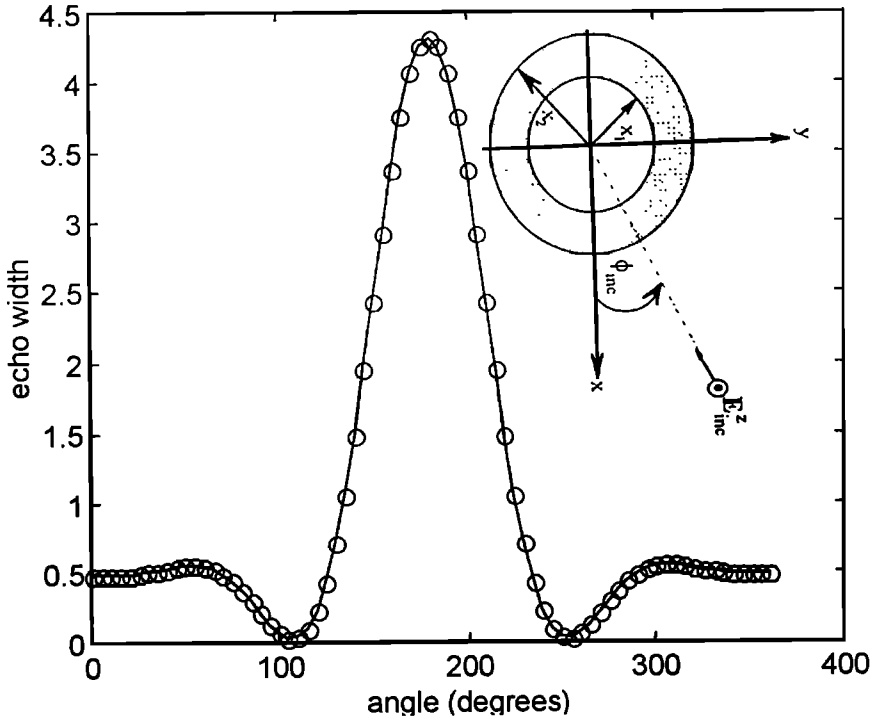

Figure 3. Dielectric circular shell, where $x_1 = 0.5\pi$, $x_2 = 0.6\pi$, $\varepsilon_r = 4$, $\sigma = 0$, and $\phi_{inc} = 0$. solid line indicates state space, and circles indicate Eigenfunction.

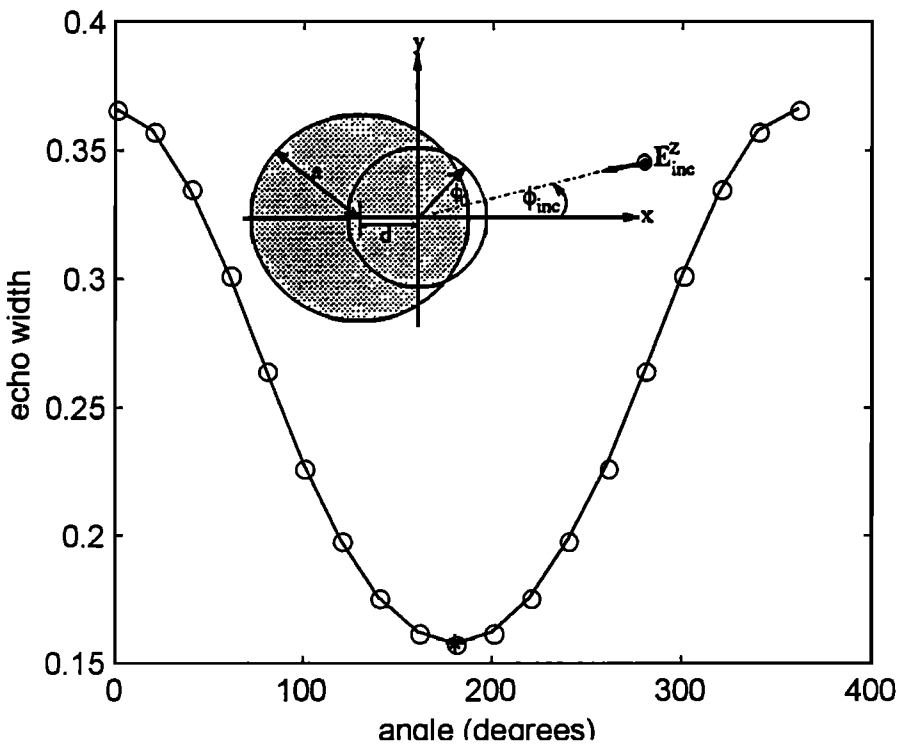

Figure 4. Off-centered circular dielectric cylinder, where $a = 1$, $d = 0.5$, $\varepsilon_r = 2$, $\sigma = 0$, and $\phi_{inc} = \pi$. Solid line indicate state space, and circles indicate analytical solution.

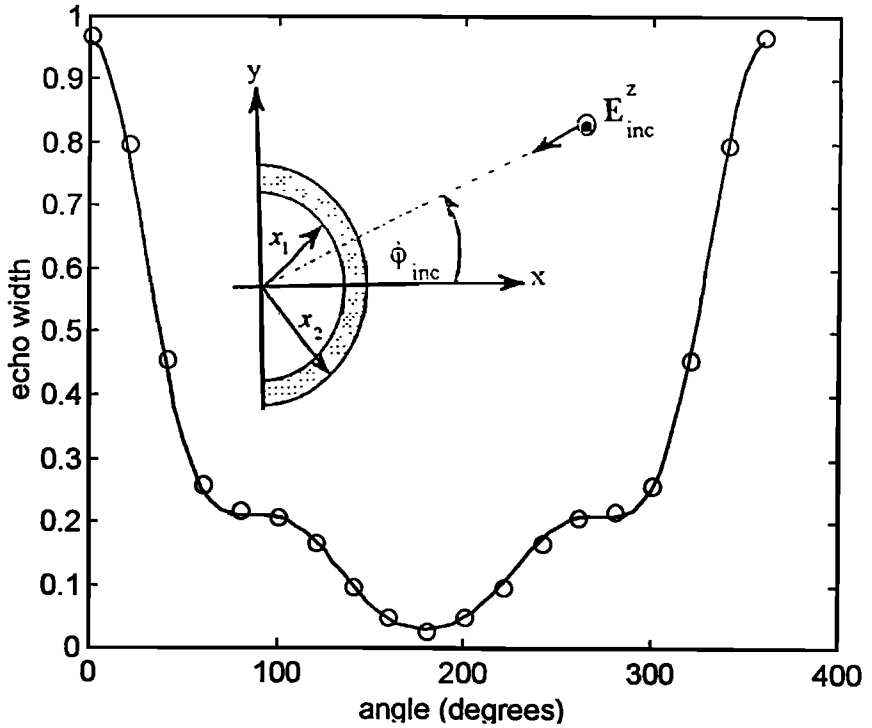

Figure 5. Semicircular dielectric ring, where $x_1 = 0.5\pi$, $x_2 = 0.6\pi$, $\varepsilon_r = 4$, $\sigma = 0$, and $\phi_{inc} = \pi$. Solid line indicates state space, and circles indicate data from *Richmond* [1965].

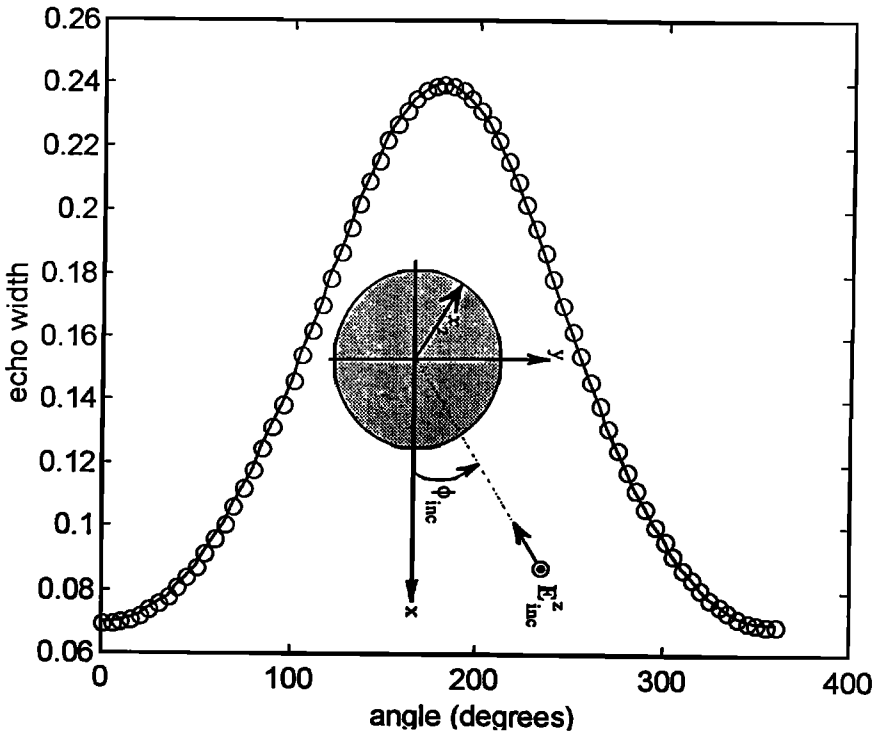

Figure 6. Luneburg lens, where $x_1 = 0$, $x_2 = 0.4\pi$, $\varepsilon_r = 2 - x^2/x_2^2$, $\sigma = 0$, and $\phi_{inc} = 0$. Solid line indicates state-space, and the circles indicate the boundary condition transfer method.

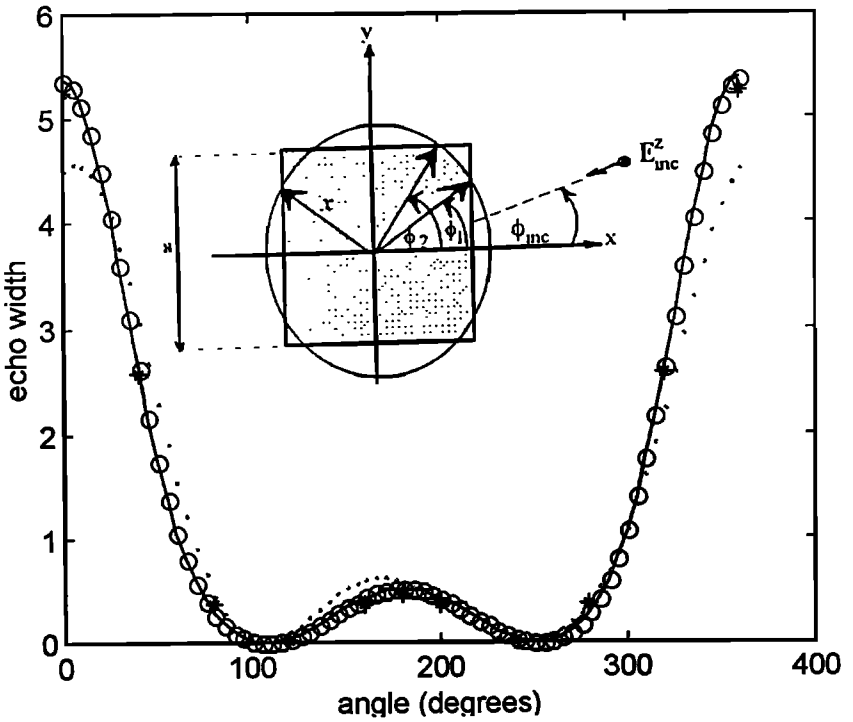

Figure 7. Square dielectric cylinder (convergence), where $a = 1.2\pi$, $\varepsilon_r = 2$, $\sigma = 0$, and $\phi_{inc} = \pi$. Solid line indicates N=5, large circles indicate N=4, small circles indicate N=3, and asterisks indicate unimoment.

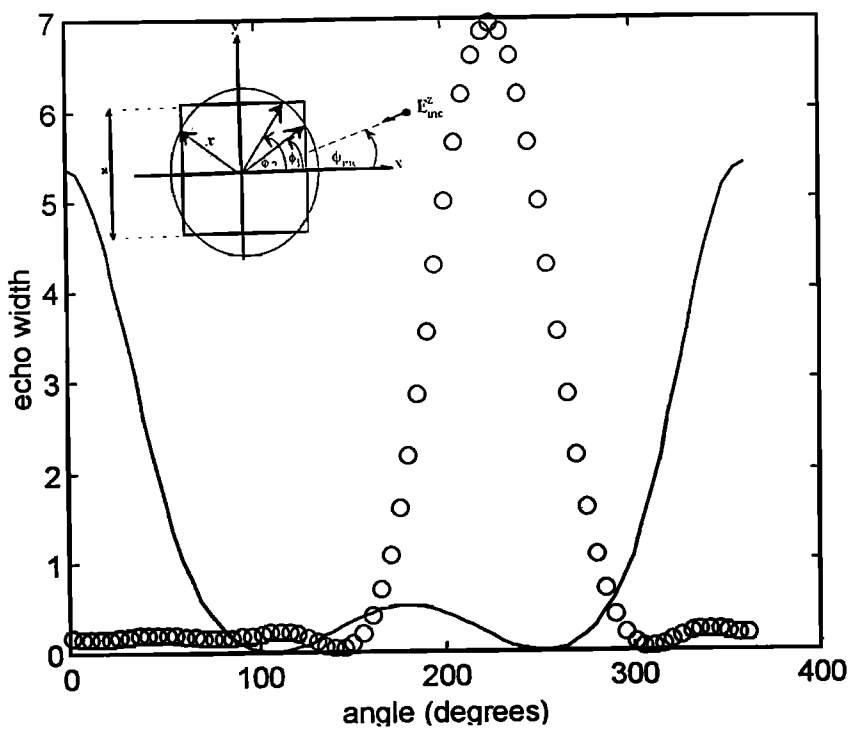

Figure 8. Square dielectric cylinder, where $a = 1.2\pi$, $\varepsilon_r = 2$, and $\sigma = 0$. Solid line indicates $\phi_{inc} = \pi$, and circles indicate $\phi_{inc} = \pi/4$.

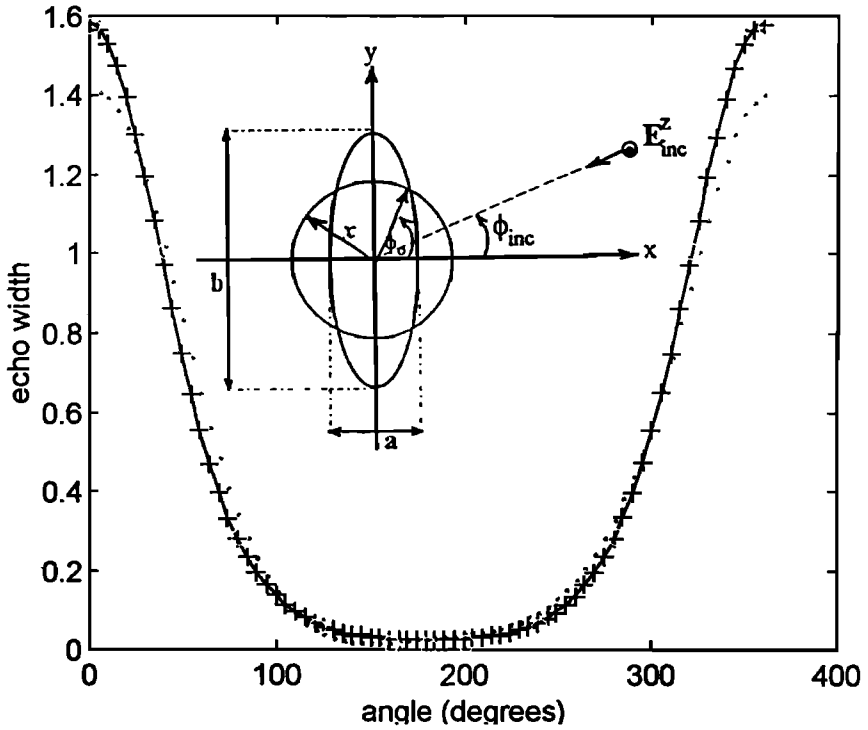

Figure 9. Elliptic dielectric cylinder (convergence), where $a = 0.4\pi$, $b = 0.6\pi$, $\varepsilon_r = 2$, $\sigma = 0$, and $\phi_{inc} = \pi$. Solid line indicate N=5, plus signs indicate N=4, small circles indicate N=3, and large circles indicate unimoment.

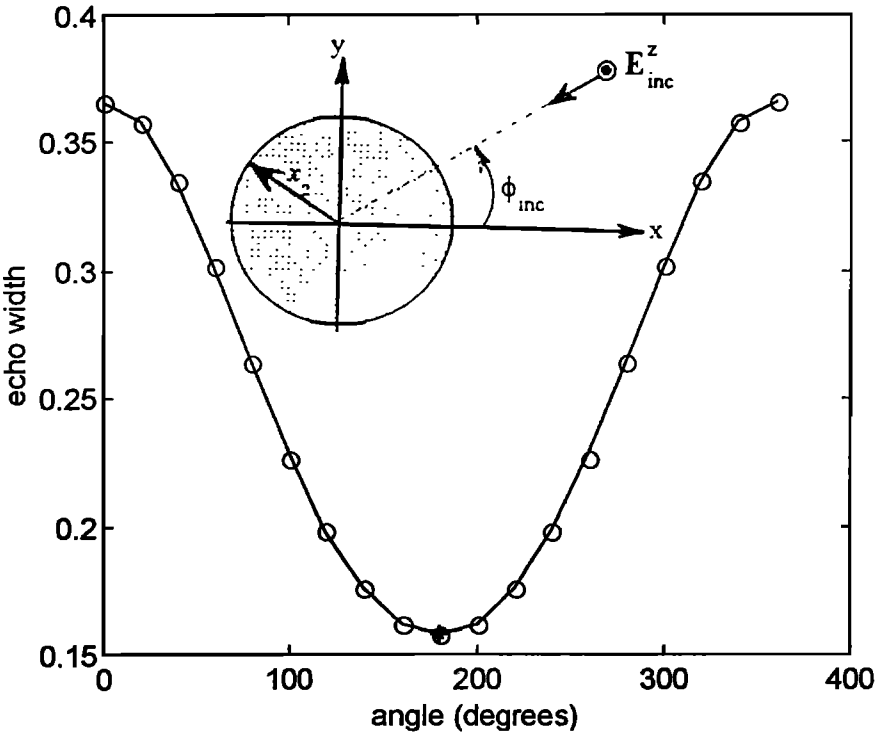

Figure 10. Lossy circular dielectric cylinder, where $f = 300\,MHz$, $x_2 = 1.26\pi$, $\varepsilon_r = 4$, $\sigma = 0.05$, and $\phi_{inc} = \pi$. Solid line indicates state-space, circles indicate boundary condition transfer method, and asterisk represents *Wu* and *Tsai* [1977].

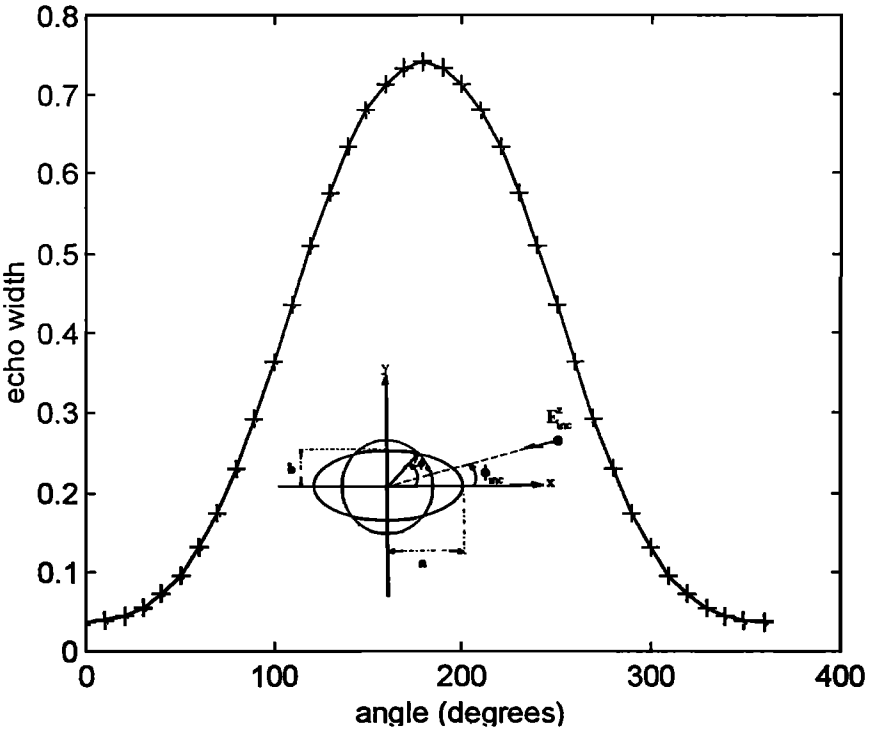

Figure 11. Lossy dielectric elliptic cylinder (convergence), where $a = 2$, $b = 1$, $\varepsilon_r = 4$, $\sigma = 0.1$, $\phi_{inc} = 0$, and $f = 300\,MHz$. Solid line indicates N=5, plus signs indicate N=3, and dots indicate N=2.

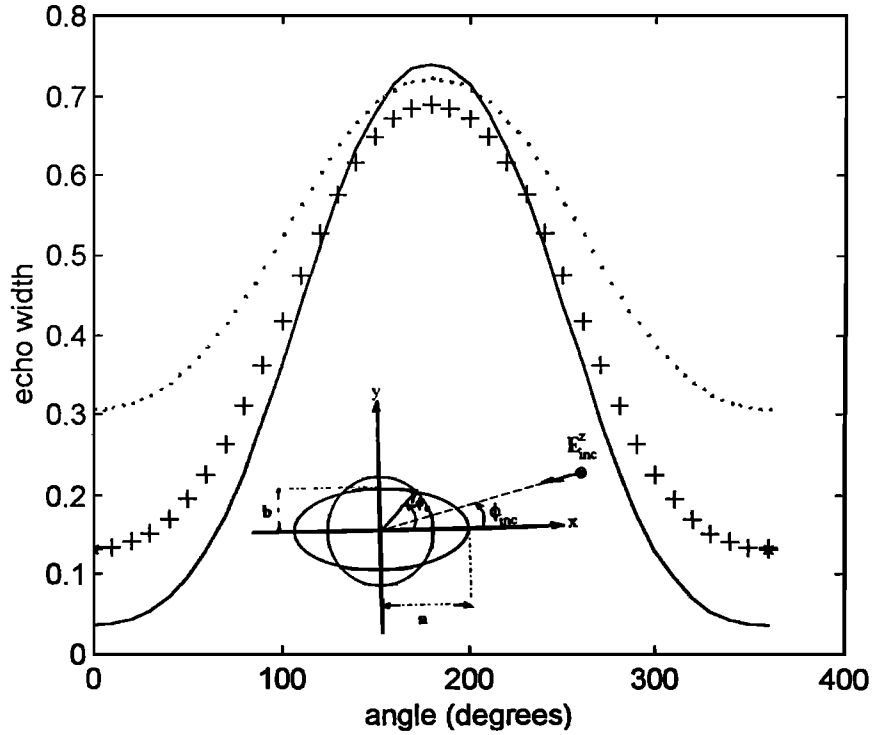

Figure 12. Lossy dielectric elliptic cylinder, where $a = 2$, $b = 1$, $\varepsilon_r = 4$, $\sigma = 0.1$, $\phi_{inc} = 0$, and $f = 300\,MHz$. Solid line indicates $\sigma = 0.1$, plus signs indicate $\sigma = 0.01$, dotted line indicates $\sigma = 0.001$, and asterisks denote *Wu and Tsai* [1977] ($\sigma = 0.01$).

The next cross-sectional shape considered is a half-circular dielectric shell of constant permittivity. Figure 5 shows the comparison between *Richmond*'s [1965] results, which are obtained by the method of moments, and the results obtained by the state-space method. The agreement is very good. As an example of a scatterer having a variable permittivity on the cross section, we considered a Luneburg lens excited with a plane wave. The results obtained were compared with those found by the boundary condition transfer method [*Tosun*, 1994]. This comparison is shown in Figure 6, with good agreement. Figures 7 and 8 show the comparison between unimoment [*Change and Mei*, 1976] and state-space methods for a dielectric cylinder of square cross section for different incident angles of a plane wave. Also shown in Figures 7 and 8 is the convergence behavior of the state-space method for various truncation numbers. An elliptic cross-sectioned dielectric cylinder under plane wave excitation conditions was also considered. The results are compared with those found by the unimoment method in Figure 9. The convergence test is also shown.

Results for a lossy circular cylinder obtained with the state-space method were found to be in excellent agreement with those found with the boundary condition transfer method [*Tosun*, 1994] (Figure 10).

We also considered a lossy elliptic cylinder excited with a plane wave. The convergence test results are given in Figure 11. Figure 12 shows the results for different values of scatterer conductivity and the comparison with *Wu and Tsai* [1977], which shows very good agreement.

5. Conclusion

The problem of electromagnetic scattering by penetrable bodies has been formulated as a reradiation problem using the volume equivalence theorem. A set of linear differential equations is obtained for the position-dependent expansion coefficients of the unknown electric field. This system is in the state-space form, for which highly developed and efficient solution techniques are available. The cross-sectional shape of the cylindrical scatterers is introduced into the calculations through the so-called shape factors, which arise in the elements of the characteristic matrix of the system of differential equations. The formulation is actually a two-point boundary value problem. In actual solution, however, only initial-value problems need to be solved. Numerical evaluation of the state-transition matrix and the zero-state response are such initial-value calculations.

The state-space method can treat scatterers which are quite inhomogeneous in their material composition and complicated in their geometrical details. However complicated these factors are, the only changes occur in the elements of the characteristic matrix [**Y**]; the field representation in terms of Bessel and Hankel functions (of real argument) and the solution procedure to find the scattering coefficients all remain unchanged. If the cross-sectional shape C is known analytically, in other words, if the polar equation of C is known, then the shape factors are found by evaluating an integral. If the complex permittivity function varies in C, this integral is calculated numerically.

The fields are actually represented by a weighted sum of cylindrical harmonics. The weights arrange themselves according to where the fields are evaluated. In other words, the weights are position-dependent scattering coefficients. Their variation with the radial variable ρ exposes the complete information about the scattering process.

A further numerical elaboration of the state-space method for both TM and TE scattering is under investigation and is hoped to be presented in a future paper.

The state-space method is intended to have a place of its own in the large spectrum of solution techniques for electromagnetic scattering by dielectric cylinders of arbitrary cross section.

References

Bates, R.H.T., and F.L. Ng., Polarization source formulation of electromagnetic fields, *Proc. IEEE, AP-20,* 1568-1574, 1972.

Cangellaris, A.C., and R. Lee, The bymoment method for two dimensional electromagnetic scattering, *IEEE Trans. Antennas Propag. AP-38*, 1429-1437, 1990.

Change, S.K., and K.K. Mei, Application of the uni-moment method to electromagnetic scattering by dielectric cylinders, *IEEE Trans. Antennas Propag. AP-24,* 35-41, 1976.

Harrington, R.F., *Time-Harmonic Electromagnetic Fields*, McGraw-Hill, New York, 1961.

Hizal, A., and H. Tosun, State-space formulation of scattering with application to spherically symmetric objects, *Can. J. Phys.*, 51, 549-558, 1973.

Leviatan, Y., and A. Boag, Generalized formulations for electromagnetic scattering from perfectly conducting and homogeneous material bodies -Theory and numerical solution, *IEEE Trans. Antennas Propag., AP-36*, 1722-1743, 1988.

Okuno, Y., The mode-matching method, in *Analysis Methods*

for Electromagnetic Wave Problems, edited by E. Yamashita, pp. 107-137, Artech House, Norwood, Mass., 1990.

Richmond, J.H., Scattering by a dielectric cylinder of arbitrary cross-section shape, *IEEE Trans. Antennas* and *Propag., AP-13*, 334-341, 1965.

Riechers, R. G., The application of lanczos S-expansion method to the solution of TM scattering from a dielectric cylinder of arbitrary cross-section, *IEEE Trans. Antennas propag., AP-38*, 1204-1212, 1990.

Shafai, L., Electromagnetic fields in the presence of cylindrical objects of arbitrary physical properties and cross-sections, *Can. J. Phys.*, 48, 1789-1798, 1970.

Shafai, L., Scattering by cylindrically symmetric objects, method of phase and amplitude functions, *Int. J. Electromagn., Theor. Exp. First Ser.*, 31, 117-125, 1971.

Shigesawa, H., The equivalent source method, in *Analysis Methods for Electromagnetic Wave Problems,* edited by E. Yamashita, pp. 177-211, Artech House, Norwood, Mass., 1990.

Tosun, H., Novel differential formulation of electromagnetic scattering by dielectric cylinders of arbitrary cross-section, *IEE Proc. Microwaves Antennas Propag.*, 141, 1994.

Wu, T., and L. L. Tsai, Scattering by arbitrarily cross-sectioned layered lossy dielectric cylinders, *IEEE Trans. Antennas Propag., AP-24,* 518-524, 1977.

N. A. Abu Zaid, A. Y. Niazi, H. Tosun, Department of Electrical and Electronic Engineering, Eastern Mediterranean University, Gazimagusa, Mersin 10, Turkey. (e-mail: nzaid@eenet.ee.emu.edu.tr; oztoprak@cc.emu.tr; haluk@eenet.ee.emu.edu.tr)

(Received March 11, 1997; revised April 20, 1998; accepted September 3,1998.)